Check for updates

*Original research article*

MEASUREMENT AND CONTROL

Measurement and Control
1–15
© The Author(s) 2026
Article reuse guidelines:
sagepub.com/journals-permissions
DOI: 10.1177/00202940261442256
journals.sagepub.com/home/mac
Sage

# Enhanced DC motor speed regulation using two-degree-of-freedom PID controller tuned by animated oat optimization with simulation and real-time experimental validation

**Gökhan Yüksek[1], Serdar Ekinci[2], Davut Izci[3,4], Rıdvan Fırat Çınar[5], Timur Lale[1], Mohit Bajaj[6,7,8], Vojtech Blazek[9] and Ievgen Zaitsev[10]**

## Abstract

This paper proposes a novel intelligent control framework for precise speed regulation of DC motors using a two-degree-of-freedom proportional–integral–derivative (2-DOF PID) controller whose six parameters are optimally tuned via the animated oat optimization (AOO) algorithm. AOO is a nature-inspired metaheuristic derived from the hygroscopic seed dispersal behavior of Avena sterilis L., offering a hybrid global-local search strategy that balances exploration and exploitation through mechanisms such as eccentric rotation, projectile jumps, and Lévy flights. The controller parameters are optimized within bounded physical limits using a composite cost function that integrates Integral Absolute Error (IAE) and normalized overshoot percentage. Comparative simulations are conducted against four recent metaheuristics, catch fish optimization algorithm (CFOA), greater cane rat algorithm (GCRA), RIME optimization, and particle swarm optimization (PSO), under identical settings (100 iterations, 30 agents). Statistical analysis over 25 independent runs reveals that the AOO algorithm achieves the best average cost value (65.2185) with the lowest standard deviation (1.2091), indicating high convergence stability. In time-domain analysis, the AOO-based 2-DOF PID controller exhibits the shortest rise time (0.9217 s), fastest settling time (1.4143 s), lowest overshoot (0.5688%), and negligible steady-state error ($\sim 10^{-13}$), outperforming all benchmark algorithms. The controller's robustness and adaptability are further validated through simulations under random reference inputs, multistep transitions, and external disturbances with measurement noise. Experimental validation using a real-time hardware-in-the-loop setup, including a Pololu 12 V DC geared motor, IBT-2 H-bridge driver, Arduino Uno, and MATLAB/Simulink interface, confirms the simulation results, demonstrating fast, stable, and accurate speed tracking across diverse reference profiles. These findings confirm that the AOO-based 2-DOF PID controller offers a highly effective, reliable, and practically deployable solution for high-performance motor control under dynamic and uncertain operating conditions.

[1]Department of Electrical and Electronics Engineering, Batman University, Turkey
[2]Department of Computer Engineering, Bitlis Eren University, Turkey
[3]Department of Electrical and Electronics Engineering, Bursa Uludag University, Turkey
[4]Applied Science Research Center, Applied Science Private University, Amman, Jordan
[5]Department of Computer Engineering, Batman University, Turkey
[6]Department of Electrical Engineering, Graphic Era (Deemed to be University), Dehradun, India
[7]Hourani Center for Applied Scientific Research, Al-Ahliyya Amman University, Amman, Jordan
[8]Graphic Era Hill University, Dehradun, India
[9]ENET Centre, CEET, VSB-Technical University of Ostrava, Czech Republic
[10]Center for Information-Analytical and Technical Support of Nuclear Power Facilities Monitoring, National Academy of Sciences of Ukraine, Kyiv, Ukraine

**Corresponding authors:**
Mohit Bajaj, Department of Electrical Engineering, Graphic Era (Deemed to be University), Dehradun 248002, India.
Email: mohitbajaj.ee@geu.ac.in

Ievgen Zaitsev, Center for Information-Analytical and Technical Support of Nuclear Power Facilities Monitoring, National Academy of Sciences of Ukraine, Akademika Palladina Avenue, 34-A, Kyiv, Ukraine.
Email: zaitsev@i.ua

Creative Commons Non Commercial CC BY-NC: This article is distributed under the terms of the Creative Commons Attribution-NonCommercial 4.0 License (https://creativecommons.org/licenses/by-nc/4.0/) which permits non-commercial use, reproduction and distribution of the work without further permission provided the original work is attributed as specified on the SAGE and Open Access pages (https://us.sagepub.com/en-us/nam/open-access-at-sage).

**Keywords**
animated oat optimization, DC motor control, experimental validation, metaheuristic optimization, PID tuning, real-time implementation, speed regulation, two-degree-of-freedom PID

Received: 16 December 2025; accepted: 17 March 2026

## Introduction

Proportional-integral-derivative (PID) controllers have been widely used in industrial control systems for many years due to their structural simplicity, intuitive settings, and successful performance in a diverse range of applications.[1] However, despite their popularity, traditional PID controllers struggle to cope with challenges such as changing loads over time, external disturbances, or the need for fast yet accurate reference tracking. These failures, which stem from the interdependence of proportional, integral, and derivative actions within a single-loop feedback structure, prevent the controller from independently adjusting its transient and steady-state responses. As a result, traditional PID controllers are often unable to meet the high-performance demands of DC motor speed control under dynamic conditions.[2–4] To overcome the limitations of classic PID structures, a two-degree-of-freedom PID controller (2-DOF PID) is developed as an extended structure that increases design flexibility. The 2-DOF PID structure separates reference tracking and disturbance rejection responses with weight parameters. The reference input is modulated by the setpoint weight coefficients applied to the proportional and derivative paths, enabling the transient response to be independently shaped without compromising steady-state regulation. This reduces excessive oscillations caused by sudden setpoint changes while maintaining aggressive corrective measures against external disturbances.[5–7] Despite these advantages, the effective implementation of 2-DOF PID controllers largely depends on the precise adjustment of numerous interrelated parameters. As system dynamics become more nonlinear or time-varying, this requirement becomes increasingly complex.[8–10]

The effectiveness of a 2-DOF PID controller depends on the correct selection of its six basic parameters: proportional, integral, and derivative gains, as well as setpoint weighting and derivative filtering coefficients. Unlike traditional PID tuning, the tuning of 2-DOF PID controllers offers an interconnected and higher-dimensional search space.[11–13] In real-world systems, manual or empirical tuning methods often fail to provide satisfactory results, especially in nonlinear systems, under varying loads, or in the presence of external disturbances. In addition, analytical tuning methods consider systems as linear and time-invariant models, and they do not investigate non-idealities in practical control systems. Hence, advanced optimization-based tuning approaches that are capable of effective search in high-dimensional parameter spaces and handle time-varying system conditions are employed.[13–15]

To address the limitations of traditional manual and analytical tuning methods, metaheuristic optimization techniques are established as promising tools for controller parameter tuning in recent years. These methods allow the use of flexible and non-derivative search strategies that are appropriate for high-dimensional, nonlinear, and multi-modal optimization problems and are inspired by natural, biological, or physical processes. Metaheuristics such as particle swarm optimization (PSO),[16] honey badger optimization algorithm (HBOA),[17] and dragonfly algorithm (DA)[18] have shown promising results in several control engineering problems. By stochastically searching the parameter space using collective intelligence or adaptive mechanisms, these techniques are capable of converging to superior parameter sets that can produce enhanced performance and robustness in comparison with classical methods. Nevertheless, although they have achieved success, commonly adopted metaheuristics frequently face the challenges of early convergence, high sensitivity to control parameters, and insufficient exploration in complicated environments.[19]

Metaheuristic algorithms are capable of providing a general framework to optimize controllers, but many established methods experience difficulty in balancing exploration and exploitation.[20–22] Classical algorithms tend to prematurely converge and become trapped in local optima, especially when working on narrow global basins or deceptive domains. Therefore, these algorithms may show unstable performance for different problem instances or require a large amount of parameter tuning. Consequently, their transferability to real-time or adaptive control applications is compromised.[23] Hence, novel optimization techniques are still required to provide more stable convergence characteristics, parameter insensitivity, and strong global search ability in tuning complex advanced controller structures.

Although numerous research studies have been carried out for PID-based motor control, reviews show that classical tuning methods cannot effectively handle the high-dimensional and nonlinear structure of new types of controllers. Manual tuning approaches are usually time-consuming with limited performance in real-time systems, and do not generalize well under different load dynamics or load changes and disturbances. In addition, the real-time 2-DOF PID tuning problem has not been adequately addressed in the literature, indicating that a flexible, noise-resilient, and globally convergent optimization method for real-time 2-DOF PID tuning still does not exist. This requires the development of a new optimization technique capable of simultaneously tuning all six coupled parameters of the

2-DOF PID controller in a reliable manner, while ensuring excellent tracking performance, fast convergence rate, and strong robustness against unmodeled dynamics and measurement noise.

In this paper, a new and intelligent control method for high-precision speed control of a DC motor is proposed by integrating the animated oat optimization (AOO) technique with a 2-DOF PID controller. The 2-DOF PID design, which is given in more detail in the following, can be seen as a multi-dimensional tuning problem, since it offers a unique opportunity to separately design each side of the controller through a total of six linked parameters. To this end, our present strategy utilizes the AOO technique, a new metaheuristic algorithm that imitates the hygroscopic spreading behavior of Avena sterilis L (ASL) seeds. This algorithm mimics potential energy-based fluctuations and biologically inspired energy-based jumping processes to move from one solution to another solution in the parameter space, and it provides an adaptive balance between global and local searching in the parameter space.

In the proposed methodology, AOO optimizes all six parameters of the controller at once within the given practical limits by minimizing a weighted sum of two metrics in the form of the product of the Integral Absolute Error (IAE) and the fraction of the normalized overshoot. Significant simulation results prove that the AOO-based controller is superior to four state-of-the-art metaheuristics in terms of all important performance indices. The AOO-based controller shows the minimum average cost (65.2185), the fastest rise time (0.9217 s), the smallest settling time (1.4143 s), and the least overshoot (0.5688%) among all methods under test. Moreover, its robustness and flexibility are also tested with multistep and stochastic references, as well as sensor noise and perturbations.

To verify real-world applicability, real-time implementation is carried out on a 12 V geared DC motor with Arduino hardware and MATLAB/Simulink interfacing. The experimental results are consistent with the simulation results, demonstrating good speed tracking ability, fast transient response, and strong disturbance rejection under practical environments. These results demonstrate that the AOO-based 2-DOF PID controller is an effective solution for intelligent motor control in dynamic and uncertain environments and also possesses high computational efficiency and robustness.

## Animated oat optimization algorithm

The AOO is a metaheuristic algorithm among nature-based algorithms and is biologically inspired by the seed dispersal of the ASL plant. ASL shows distinctive hygroscopic motions due to deformation of the primary barley in response to moisture changes. Such movements contribute to the transportation of seeds across different landscapes and follow stochastic and energy-based dispersal patterns. These behaviors are exploited as the exploration and exploitation stages in the proposed optimization scheme.

### Initialization phase

The algorithm begins by initializing a population of $N$ candidate solutions across a $Dim-dimensional$ search space. The population matrix $X$ is defined as equation (1):

$$X = \begin{bmatrix} x_{1,1} & x_{1,2} & \ldots x_{1,Dim} \\ x_{2,1} & x_{2,2} & \ldots x_{2,Dim} \\ \vdots & \vdots & \ddots \quad \vdots \\ x_{N,1} & x_{N,2} & \cdots x_{N,Dim} \end{bmatrix} \tag{1}$$

Each variable $x_{i,j}$ is randomly initialized within its respective bounds according to equation (2):

$$x_{i,j} = r \cdot \left(UB_j - LB_j\right) + LB_j, i = 1, 2, \ldots, N, j = 1, 2, \ldots, Dim \tag{2}$$

where $r \in [0, 1]$ is a uniformly distributed random number and $UB_j$, $LB_j$ are the upper and lower bounds of the $j_{th}$ dimension, respectively.

### Parameter calculation

Inspired by the physical traits of animated oat seeds, algorithm parameters are dynamically adjusted during execution. These parameters include mass ($m$), awn length ($L$), eccentricity coefficient ($e$), and the convergence control factor ($c$) as equation (3):

$$m = 0.5 \cdot \frac{r}{Dim}, L = N \cdot \frac{r}{Dim}, e = 0.5 \cdot \frac{r}{Dim}, c = 1 - \left(\frac{t}{T}\right) \tag{3}$$

where $t$ is the current iteration, and $T$ is the maximum number of iterations.

### Exploration phase

The global search ability of AOO is modeled after wind-, water-, and animal-driven seed dispersion, introducing randomness in positional updates as equations (4) and (5):

$$W = \frac{c}{\pi} \cdot (2r - 1) \bigotimes UB \tag{4}$$

$$X_{t+1}(i) = \begin{cases} \frac{1}{N}\sum_{j=1}^{N} X_t(j) + W, if\ mod\ (i, N/10) = 0 \\ X_{best} + W, if\ mod\ (i, N/10) = 1 \\ X_t(i) + W, otherwise \end{cases} \tag{5}$$

This approach allows seeds to randomly scatter in a large region of the search space, thereby enhancing diversity.

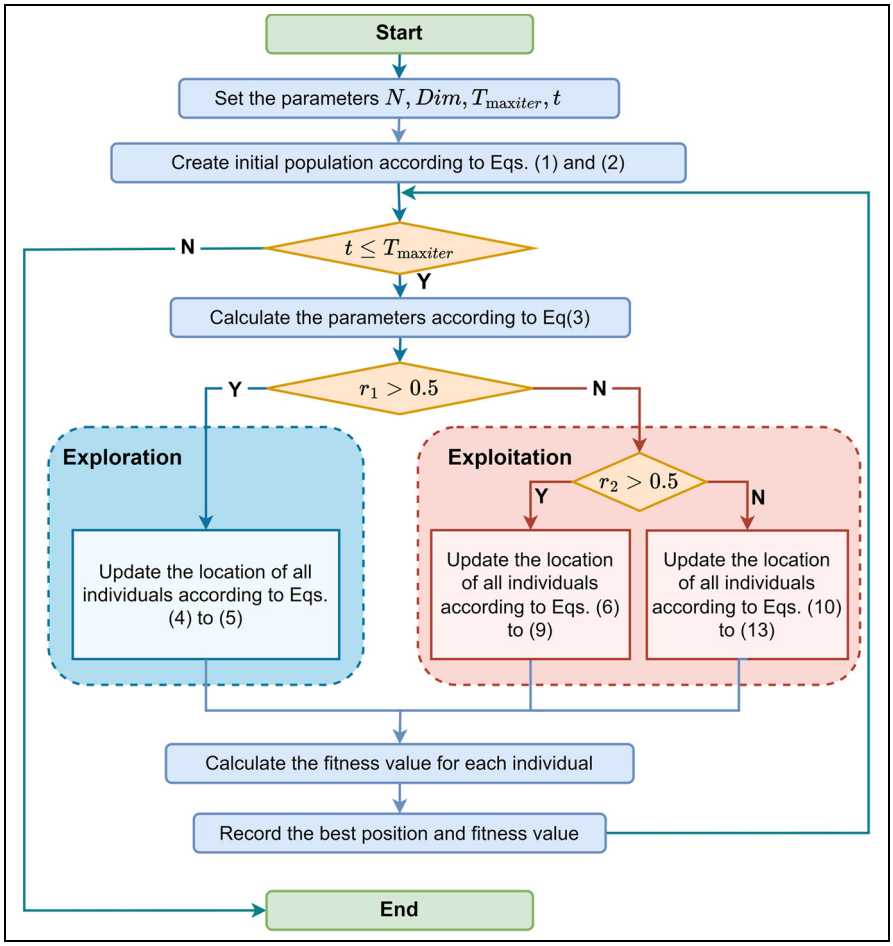



**Figure 1.** AOO flowchart.

### *Exploitation phase*

When no obstacles are encountered, seed rolling induced by hygroscopic tension is modeled using eccentric rotation and Levy flights as equations (6)–(9):

$$A = UB - \left| UB \cdot t \cdot \frac{\sin(2\pi r)}{T} \right| \tag{6}$$

$$R = \left(m \cdot e + L^2\right) \cdot rand(-A, A)/Dim \tag{7}$$

$$Levy(\beta) = 0.01 \cdot \frac{\mu \cdot \sigma}{|v|^{1/\beta}}, \beta = 1.5 \tag{8}$$

$$X_{t+1}(i) = X_{best} + R + c \cdot Levy(\beta) \otimes X_{best} \tag{9}$$

This mechanism promotes local refinements in promising regions of the solution space, inspired by anisotropic swelling and torque-induced motion in oat seeds. When physical barriers are simulated, the stored energy in the seed's awn is assumed to be released, resulting in an ejection behavior modeled as projectile motion as equations (10)–(13):

$$B = UB - \left| UB \cdot t \cdot \frac{\cos(2\pi r)}{T} \right| \tag{10}$$

$$k = 0.5 + 0.5r, x = 3r/Dim, \theta = \pi r, \alpha = \frac{e^{r'/T}}{\pi} \tag{11}$$

$$J = \frac{2kx^2 \sin(2\theta)}{mg} \cdot rand(-B, B) \cdot (1 - \alpha)/Dim \tag{12}$$

$$X_{t+1}(i) = X_{best} + J + c \cdot Levy(\beta) \otimes X_{best} \tag{13}$$

This mechanism enhances the algorithm's capacity to escape local optima by emulating abrupt directional jumps.

### *Algorithmic characteristics*

Each iteration involves probabilistic selection between exploration and two types of exploitation operators as shown in the flowchart of AOO in Figure 1. The design ensures dynamic adaptation between wide-range search and focused exploitation. The overall time complexity is given by equation (14):

$$O(T \cdot N \cdot (D + COF)) \tag{14}$$

where $COF$ is the cost of one fitness function evaluation, $D$ is the problem dimensionality, $N$ is the population size, and $T$ is the maximum number of iterations. The space complexity is as equation (15):

$$O(D \cdot N + T) \tag{15}$$

Due to its reliance on biologically grounded motion dynamics and its hybrid treatment of search phases, AOO is distinguished by its robustness, search efficiency, and capacity to maintain solution diversity over time.

### *Relation to existing metaheuristic search strategies*

In recent years, a variety of nature-inspired metaheuristic algorithms have incorporated stochastic motion patterns to enhance search diversity and avoid premature convergence. Among these mechanisms, Lévy-flight-based perturbations have been employed in different optimization frameworks as an auxiliary strategy to improve exploration capability. Nevertheless, the presence of such stochastic components does not, by itself, define the core search philosophy or structural characteristics of an optimization algorithm.

The AOO is inspired by the hygroscopic motion and energy accumulation and release behavior observed in ASL seeds. Instead of approaches that metaphorically model reproduction, replacement, or elimination of individuals, AOO captures physical dynamics of motion, such as long-range dispersal, eccentric rolling induced by anisotropic swelling, and sudden projectile-like motion due to the release of stored elastic energy. These operators control the exploration-exploitation balance at the search level during the optimization process.

Lévy-flight perturbations used in AOO are limited to the role of an optional refinement mechanism to improve local search ability and to escape from poor local solutions within the AOO framework. The prevailing search mode is steered by energy-based mechanical motion operators, a feature that sets AOO apart from other nature-inspired algorithms, where Lévy flights represent the primary search engine. Accordingly, this allows proper and stable convergence, which are favorable properties for constrained high-dimensional problems such as multi-parameter controller tuning.

## Mathematical modeling of DC motor

In modeling the dynamic behavior of a DC motor, the magnetic field remains constant throughout the operation. Under this condition, which is valid for systems using permanent magnets or externally excited field windings, the torque produced by the motor is linearly dependent on the armature current.[24–26] The torque–current relationship is expressed as equation (16):

$$T(t) = K_t \cdot i(t) \tag{16}$$

where $T(t)$ is the generated electromagnetic torque, $i(t)$ is the armature current, and $K_t$ denotes the motor torque constant in $Nm/A$. As the rotor spins within the magnetic field, an electromotive force opposing the applied voltage is induced across the armature terminals. This back electromotive force (EMF) is proportional to the angular velocity $\dot{\theta}(t)$, given by equation (17):

$$e(t) = K_e \cdot \dot{\theta}(t) \tag{17}$$

Here, $K_e$ is the back EMF constant, with units of $V \cdot s/rad$. In SI-consistent formulations, it is common for $K_t$ and $K_e$ to share the same numerical value. The mechanical dynamics of the motor are derived from Newton's second law for rotational motion. When the effects of inertia and viscous damping are considered as equation (18):

$$J \cdot \ddot{\theta}(t) + b \cdot \dot{\theta}(t) = K_t \cdot i(t) \tag{18}$$

where $J$ is the moment of inertia and $b$ is the viscous friction coefficient. On the electrical side, the dynamics of the armature circuit are governed by Kirchhoff's voltage law. The total applied voltage equals the sum of voltage drops across the inductor, resistor, and back EMF as equation (19):

$$L \cdot \frac{di(t)}{dt} + R \cdot i(t) = V(t) - K_e \cdot \dot{\theta}(t) \tag{19}$$

By applying the Laplace transform, assuming zero initial conditions, the system is converted into the frequency domain as equations (20) and (21):

$$(Js + b) \cdot \dot{\Theta}(s) = K_t \cdot I(s) \tag{20}$$

$$(Ls + R) \cdot I(s) = V(s) - K_e \cdot s \cdot \Theta(s) \tag{21}$$

Eliminating $I(s)$ from the equations and choosing the armature voltage $V(s)$ as the input and the angular velocity $\dot{\theta}(\mathrm{s}) = \mathrm{s} \cdot \Theta(\mathrm{s})$ as the output, the open-loop transfer function is derived as equation (22):

$$\frac{\dot{\theta}(s)}{V(s)} = \frac{K_t}{(Js + b)(Ls + R) + K_t K_e} \tag{22}$$

This second-order transfer function characterizes the dynamic input-output behavior of an armature-controlled DC motor, serving as the basis for control design and analysis in speed regulation applications. The MATLAB/Simulink parameter estimation toolbox estimates DC motor parameters. The values obtained are shown in Table 1.

**Table 1.** DC motor parameters.

| Parameter | Symbol | Value | Unit |
|---|---|---|---|
| Moment of inertia of the rotor | $J$ | 0.013767 | $kg/m^2$ |
| Motor viscous friction constant | $b$ | 0.049813 | $N.m.s$ |
| Electromotive force constant | $K_e$ | 0.020375 | $(V/rad)/sec$ |
| Motor torque constant | $K_t$ | 0.020375 | $Nm/Amp$ |
| Electric resistance | $R$ | 0.18644 | $\Omega$ |
| Electric inductance | $L$ | 0.0063 | $H$ |

By substituting the obtained parameters into equation (22), the second-order transfer function representing the DC motor shown in equation (23) is obtained.

$$G(s) = \frac{0.02038}{0.00008673s^2 + 0.002881s + 0.009702} \quad (23)$$

## A novel control strategy for DC motor speed regulation

In this paper, an innovative approach using a 2-DOF PID controller is developed for the speed control of a DC motor, where the parameters of the PID controller are optimally tuned by the AOO algorithm. The 2-DOF PID design provides more degrees of freedom to enhance the performance of the system when tracking the reference and rejecting disturbances in comparison with the traditional PID controller. To improve the dynamic behavior and robustness with respect to parameter uncertainties, the control gains, including the setpoint weighting factors, are systematically optimized using AOO. Through this integration, the proposed scheme further reduces transient responses such as overshoot and settling time, while achieving lower steady-state error and improved accommodation of load variations compared with traditional tuning methods.

### *2-DOF PID controller for DC motor speed control system*

In the feedforward/feedback control structure, a 2-DOF PID controller is employed, as depicted in Figure 2. In the 2-DOF PID structure, the classical PID equation is modified with two extra weights, enabling the tuning of the setpoint response separately from disturbance rejection. Such flexibility is essential in time-varying processes with fast reference tracking and disturbance suppression.[7,27]

The mathematical formulation of the 2-DOF PID controller used in this study is given by equation (24):

$$U(s) = K_P[\alpha \times R(s) - Y(s)] + \frac{K_I}{s}[R(s) - Y(s)] + \frac{K_D N s}{s + N}[\beta \times R(s) - Y(s)] \quad (24)$$

where $U(s)$ is the control signal, $R(s)$ is the reference input, $Y(s)$ is the system output, $K_P$, $K_I$, $K_D$ are the proportional, integral, and derivative gains, respectively, $\alpha$ is the setpoint weighting applied to the proportional term, $\beta$ is the setpoint weighting applied to the derivative term, $N$ is the derivative filter coefficient, which determines the cutoff frequency of the low-pass filter applied to the derivative action.

In this configuration, the proportional and derivative terms are applied not directly to the error signal but to weighted differences between the reference and output signals, enhancing flexibility. Specifically, the $\alpha$ parameter allows attenuation of aggressive responses to setpoint changes by adjusting the influence of the reference signal on the proportional term. Likewise, the $\beta$ parameter modulates the sensitivity of the derivative action to the reference trajectory, thereby offering improved control over transient dynamics and reducing sensitivity to measurement noise.

The derivative term includes a first-order low-pass filter implemented through the transfer function $\frac{Ns}{s+N}$ which helps to mitigate the amplification of high-frequency noise that commonly affects pure derivative control. The integral term retains its classical form, ensuring zero steady-state error by accumulating the control error over time.

All six parameters ($K_P$, $K_I$, $K_D$, $\alpha$, $\beta$, $N$) of the controller are simultaneously optimized using the AOO algorithm. By utilizing the seed dispersal-inspired search mechanism of AOO, the controller parameters are adaptively adjusted to minimize a composite performance index that involves rise time, settling time,

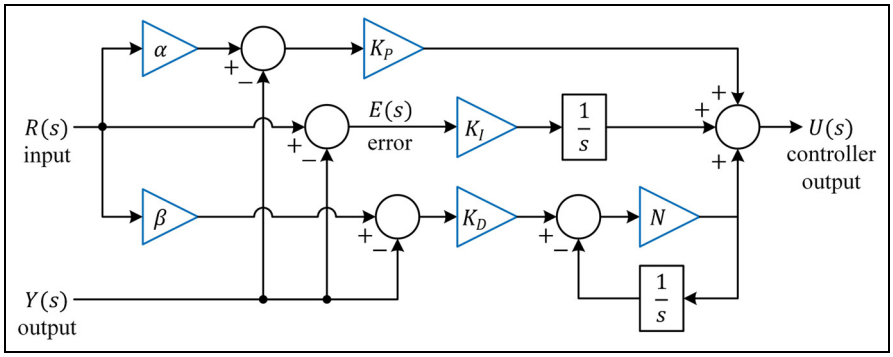



**Figure 2.** Control architecture of the 2-DOF PID regulator.

**Table 2.** Bounds of 2-DOF PID controller.

| Bound | $K_P$ | $K_I$ | $K_D$ | $N$ | $\alpha$ | $\beta$ |
|---|---|---|---|---|---|---|
| Low | 0.001 | 0.01 | 0.001 | 10 | 0.5 | 0.5 |
| Upper | 0.1 | 1 | 0.01 | 500 | 2 | 2 |

overshoot, and integral error metrics. This integration of an advanced metaheuristic with a flexible control structure enables robust and high-precision speed regulation of the DC motor under varying operating conditions.

### Developed cost function

In the optimization process of the proposed AOO-based 2-DOF PID controller, a composite cost function is defined to guide the parameter tuning performed by the AOO algorithm. The simulation time is set to $t_{final} = 20$ seconds, and the error signal $e(t)$ is used as the basis for performance evaluation. IAE is employed in this study to represent the accumulated magnitude of the control error over time.[28] The IAE is mathematically defined by equation (25):

$$IAE = \int_0^{t_{final}} |e(t)|\, dt \tag{25}$$

To incorporate both transient and steady-state characteristics into the optimization process, an adaptive cost function $CF$ is formulated as a weighted combination of the IAE and the normalized percent overshoot. $PO_{norm}$ The cost function is expressed as equation (26):

$$CF = \gamma \times IAE + (1 - \gamma) \times PO_{norm} \tag{26}$$

In this formulation, $\gamma$ denotes the weighting factor that balances the trade-off between minimizing the integral error and penalizing overshoot. In the present study, this parameter is fixed at $\gamma = 0.85$, prioritizing error minimization while still moderately accounting for overshoot suppression. The overshoot term is normalized to ensure scale compatibility within the composite function.

The optimization process is constrained within predetermined parameter bounds to ensure practical and physically realizable controller settings. These bounds are given in Table 2, covering all six tunable parameters of the controller:

The minimum and maximum values of the proportional and integral gains are chosen to avoid excessive control effort, actuator saturation, and instability, while at the same time providing sufficient authority to accurately regulate the speed. The derivative gain is intentionally limited to a small range to prevent amplification of measurement noise, which is particularly important for real-time motor control. The derivative filter coefficient is bounded to satisfy high-frequency noise attenuation and transient response requirements. The setpoint weighting parameters $\alpha$ and $\beta$ are restricted to ranges that are often used in practice for 2-DOF PID controllers, so that the reference tracking and disturbance rejection behavior may be shaped independently without causing aggressive transient behavior.

These bounds guarantee stability, implementability, and hardware compatibility of the controller parameters while allowing sufficient flexibility for the search process. By combining this bounded optimization scheme with the adaptive cost function, the proposed approach ensures that the controller is not only fast and accurate but also robust under real-world operating limitations.

It is worth mentioning that the proposed AOO-based tuning framework functions as an offline optimization method. Algorithmic evolution is characterized by iteration-dependent parameters and switching between exploration and exploitation operators to control the optimization trajectory, as opposed to modifying controller gains during real-time operation. This separation distinguishes the proposed method from online or adaptive parameter tuning schemes and guarantees physically implementable controller parameters for practical applications.

### Utilization of the AOO algorithm in the control of DC motor speed

Six controller parameters are adaptively adjusted within predefined boundaries by the AOO algorithm as shown in Figure 3. The integration of AOO into the controller's parameter detection enables significant improvements in speed-tracking accuracy, overshoot reduction, and robustness under practical operating conditions.

## Simulation and experimental results

### Metaheuristic algorithms employed for performance comparison

To evaluate the effectiveness of the proposed control strategy, the AOO algorithm is compared with four recent metaheuristic algorithms, catch fish optimization algorithm (CFOA),[29] greater cane rat algorithm (GCRA),[30] rime optimization algorithm (RIME),[31] and PSO.[32] These algorithms are selected due to their proven performance in continuous optimization problems and their recent adoption in control engineering applications. In all cases, fair benchmarking conditions are ensured by using identical simulation settings, including a maximum number of 100 iterations and a swarm size of 30 particles for each algorithm.

For AOO, no control parameters beyond the default search dynamics are used. Therefore, AOO is employed without any manual fine-tuning to avoid algorithm-specific bias and to ensure a fair comparison. All algorithms are executed using their standard or commonly

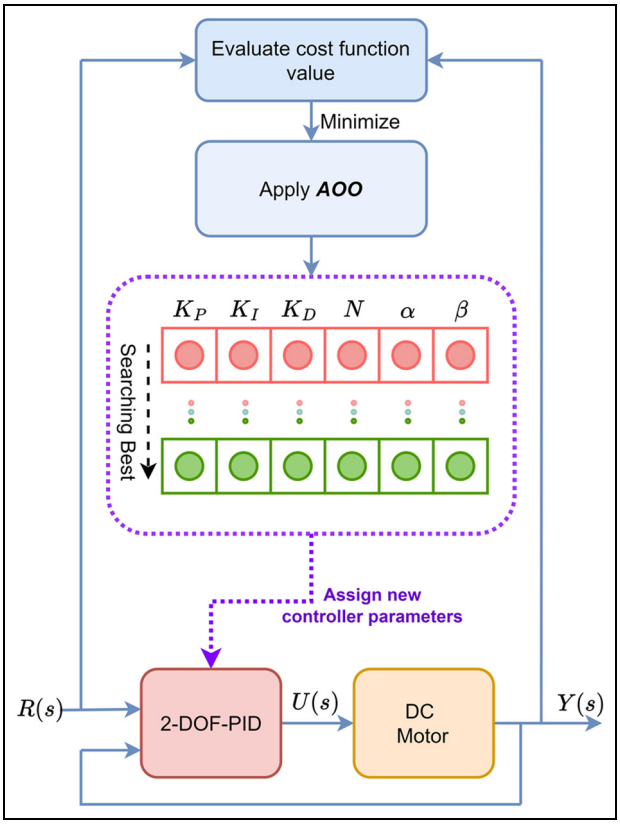



**Figure 3.** Block diagram of the AOO-based optimization framework for tuning 2-DOF PID controller parameters in DC motor control.

recommended parameter settings. CFOA and GCRA are applied with their original structures; in the case of GCRA, the control parameter $\rho$ is set to 0.5. For RIME, the internal control parameter $w$ is fixed at 5 throughout the optimization process. The PSO algorithm, used here as a standard reference, is executed with commonly adopted cognitive and social acceleration coefficients, $c_1 = 2$ and $c_2 = 2$. At the same time, the inertia weight $w$ is linearly decreased from 0.9 to 0.1 throughout the iterations to balance exploration and exploitation.

The configuration of each algorithm, including its control parameters where applicable, is summarized in Table 3. This standardized setup enables a consistent and unbiased comparison of convergence behavior and final control performance across all tested optimization methods.

## Statistical analysis

To provide a statistically reliable comparison, each optimization algorithm is independently executed 25 times under identical simulation settings. The resulting cost function values are recorded and analyzed using both graphical and statistical methods. Figure 4 presents a comparative boxplot that illustrates the

**Table 3.** Parameter settings for AOO, CFOA, GCRA, RIME, and PSO.

| Algorithm | Parameter | Value |
|---|---|---|
| AOO[33] | Maximum number of iterations | 100 |
| | Swarm size | 30 |
| CFOA[29] | Maximum number of iterations | 100 |
| | Swarm size | 30 |
| GCRA[30] | Maximum number of iterations | 100 |
| | Swarm size | 30 |
| | Control parameter $\rho$ | 0.5 |
| RIME[31] | Maximum number of iterations | 100 |
| | Swarm size | 30 |
| | Control parameter $w$ | 5 |
| PSO[32] | Maximum number of iterations | 100 |
| | Swarm size | 30 |
| | Cognitive and social constants $c_1$ and $c_2$ | 2; 2 |
| | Inertia weight $w$ | Linear reduction from 0.9 to 0.1 |

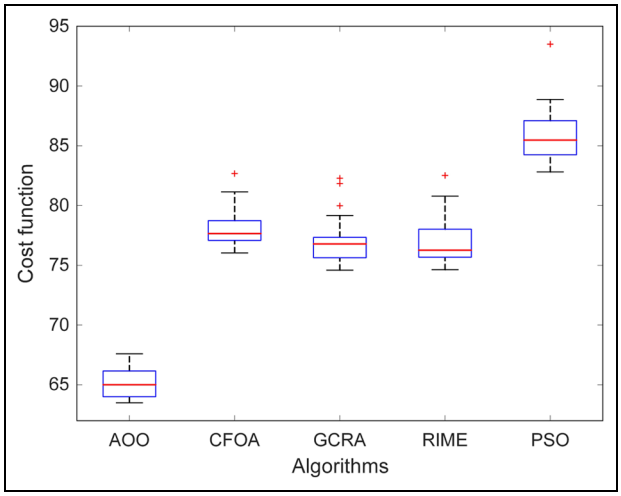



**Figure 4.** Comparative boxplot analysis.

distribution, central tendency, and spread of the cost function values for all algorithms. As observed from the plot, the AOO algorithm yields the lowest median and minimum cost values, with a notably narrower interquartile range compared to the other methods.

This indicates a consistent and stable convergence behavior with minimal dispersion across trials. Further statistical metrics for each algorithm are summarized in Table 4. The AOO algorithm achieves the best average cost function value at 65.2185, significantly outperforming CFOA (78.1763), GCRA (77.0481), RIME (76.9805), and PSO (85.8583). In terms of variability, AOO also exhibits the most minor standard deviation

**Table 4.** Statistical comparison of algorithms for minimization of *CF* cost function.

| Statistical metric | AOO | CFOA | GCRA | RIME | PSO |
|---|---|---|---|---|---|
| Average | 65.2185 | 78.1763 | 77.0481 | 76.9805 | 85.8583 |
| Standard deviation | 1.2091 | 1.6660 | 2.0551 | 1.9315 | 2.4110 |
| Median | 65.0067 | 77.6532 | 76.7864 | 76.2619 | 85.4777 |
| Minimum | 63.4955 | 76.0337 | 74.5934 | 74.6276 | 82.8112 |
| Maximum | 67.5910 | 82.6714 | 82.2840 | 82.5157 | 93.5021 |
| Rank | 1 | 4 | 3 | 2 | 5 |

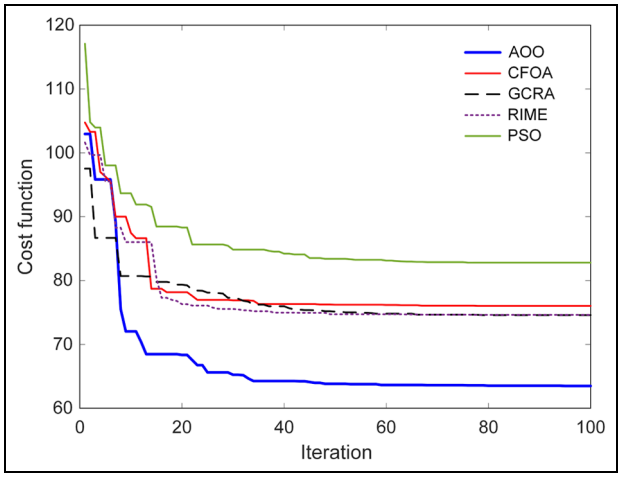



**Figure 5.** Convergence analysis.

(1.2091), demonstrating its robustness across repeated runs. It consistently ranks first in performance, with the lowest maximum and highest minimum values also belonging to AOO, reinforcing its dominance in both optimality and reliability.

These results collectively indicate that the AOO algorithm both provides superior solutions for the controller tuning problem and exhibits higher statistical stability and repeatability than the other tested metaheuristics. This strengthens the argument for its practical suitability in high-precision control applications.

## Convergence analysis

The convergence behavior of each optimization algorithm is investigated to assess its search efficiency and stability throughout the parameter-tuning process. Figure 5 illustrates the cost function trajectories over 100 iterations for AOO, CFOA, GCRA, RIME, and PSO. As observed from the convergence curves, the AOO algorithm exhibits the fastest and most stable descent toward a lower cost value compared to its counterparts. A rapid drop in the cost function is achieved within the first 20 iterations, followed by a smooth and consistent convergence to the global optimum without oscillation or stagnation.

On the other hand, other algorithms exhibit somewhat slower convergence and larger final cost values. PSO, in particular, displaying a large initial cost and early stagnation, and cannot come close to the leading solutions in terms of solution quality within the given iteration budget. RIME and CFOA manage to converge moderately, although with more fluctuation and higher variance, whereas GCRA has a more stable declining pattern but end in a local optimum. To further reinforce the analysis, the best controller parameters of each algorithm are listed in Table 5. The AOO scheme provides the best set of 2-DOF PID parameters. The variation in parameter settings among the other algorithms reflects their different convergence properties and suboptimal solutions, which further corroborates the robustness and efficiency of AOO for the DC motor speed regulation problem.

## Closed-loop response analysis

The 2-DOF PID controllers designed by various optimization methods are tested through step response simulations for the closed-loop system. From the comparative time responses in Figure 6, it is observed that all the considered controllers successfully achieve stable tracking convergence to the desired setpoint of 150 rpm. However, as shown in the zoomed view in Figure 7, the

**Table 5.** Optimal 2-DOF PID controller parameters.

| Parameter | AOO | CFOA | GCRA | RIME | PSO |
|---|---|---|---|---|---|
| $K_P$ | 0.09393 | 0.09773 | 0.06831 | 0.09851 | 0.03484 |
| $K_I$ | 0.7865 | 0.8176 | 0.7639 | 0.8714 | 0.7192 |
| $K_D$ | 0.001034 | 0.001592 | 0.002937 | 0.002487 | 0.001794 |
| $N$ | 151.3917 | 421.9230 | 261.9956 | 834.7516 | 191.3047 |
| $\alpha$ | 1.9995 | 0.9809 | 1.6503 | 0.8369 | 1.8785 |
| $\beta$ | 0.6512 | 0.9672 | 0.6629 | 0.6893 | 0.7378 |

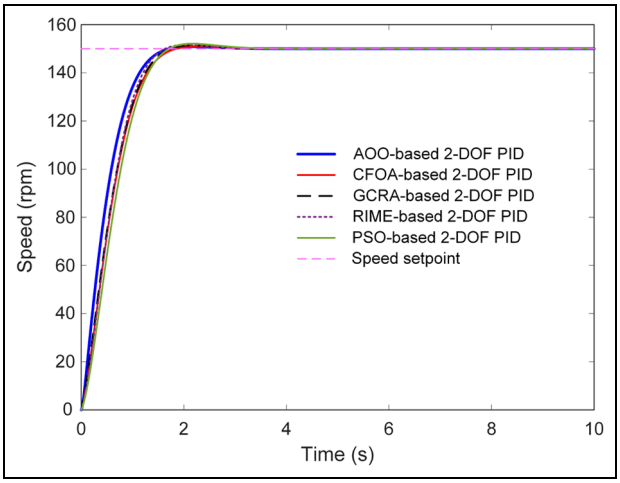



**Figure 6.** Comparative time response analysis of 2-DOF PID controlled DC motor.

response behaviors differ significantly among the methods, especially in terms of rise time, overshoot, and settling process.

The scalar performance measures derived from the simulation results are reported in Table 6. The AOO-based controller has the best overall dynamic behavior among all tested algorithms. In particular, the proposed approach provide the shortest rise time (0.9217 s) and the best settling time (1.4143 s) with the minimum overshoot (0.5688%). The AOO-based 2-DOF PID peak value remains very close to the reference value without aggravated transient amplification, and the corresponding steady-state error is practically zero, which is comparable to other approaches within numerical tolerance.

However, the PSO-based controller yields the worst performance in terms of maximum overshoot (1.4024%) and the slowest rise time (1.0367 s), representing a rather mild and oscillatory reaction. The CFOA, GCRA, and RIME approaches lead to intermediate results, with RIME having somewhat better settling performance but slightly larger overshoot compared with AOO. Under the same control structure and simulation conditions, the AOO-based 2-DOF PID method still outperforms all other candidates in terms of both transient and steady-state results, which corroborates its superiority for fast, stable, and accurate speed regulation.

It is worth noting that the speed of transient responses is deliberately moderated by the optimized controller parameters to prevent severe overshoot and oscillation. The proportional- and derivative-related parameters mainly influence the rise and settling times, whereas the integral gain contributes to minimizing the steady-state error, yielding a balanced trade-off between speed and stability under disturbances.

### *Reference input tracking performance of AOO-based 2-DOF PID controller*

To understand the reference input tracking performance of the AOO-based 2-DOF PID controller, further simulations are also carried out for the above simple command under differing conditions. The system response for a series of step changes in the reference speed is shown in Figure 8. With the aid of the proposed controller, the system is able to track every transition with negligible overshoot and converged very fast after each change. Here, the response tracks the setpoint trajectory very well, and no steady-state error is introduced during the entire simulation time of 100 s.

To evaluate the performance of the AOO-based 2-DOF PID when facing more complexity and uncertainty using a widely changing speed reference, the speed reference is randomly chosen. As can be seen from Figure 9, in the presence of short-term and unexpected variations of the input signal, the AOO-based 2-DOF PID can achieve tracking results close to the desired speed profile. The output of the system tracks the complicated reference curve very well, and the tracking error is negligible.

The obtained results suggest that the AOO-based 2-DOF PID scheme can achieve high-quality tracking for both deterministic and stochastic references. The controller provides a good stability and fast response behavior under all test conditions.

### *Under external disturbance and measurement noise*

The performance of the AOO-based 2-DOF PID controller is also tested in the presence of external disturbances and measurement noise, as shown in Figure 10. In this simulation, instantaneous torque disturbances are applied to the system at various points in time, and Gaussian white noise is added to the speed feedback signal to

**Table 6.** Comparison of time response specifications.

| Stability metric | AOO | CFOA | GCRA | RIME | PSO |
|---|---|---|---|---|---|
| Rise time (s) | 0.9217 | 1.0227 | 1.0117 | 0.9605 | 1.0367 |
| Settling time (s) | 1.4143 | 1.5576 | 1.5015 | 1.4340 | 1.5344 |
| Peak (rpm) | 150.8531 | 150.8535 | 151.4126 | 151.5632 | 152.1036 |
| Overshoot (%) | 0.5688 | 0.5690 | 0.9417 | 1.0422 | 1.4024 |
| Steady-state error (%) | 3.4106E−13 | 5.3054E−13 | 5.3054E−13 | 3.2780E−12 | 3.7327E−12 |

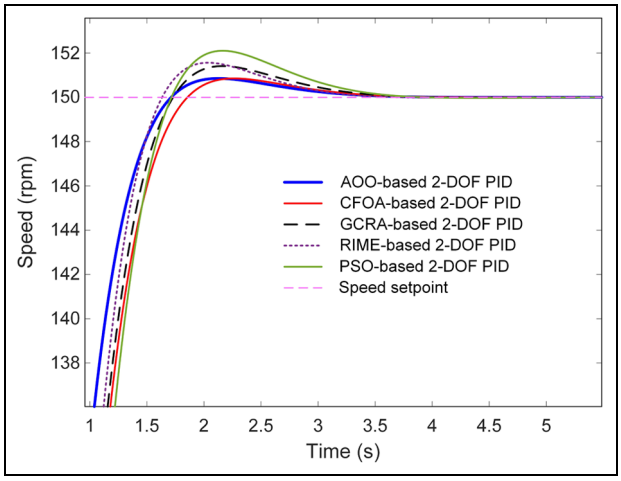



**Figure 7.** Detailed view of comparative time response analysis of 2-DOF PID controlled DC motor.

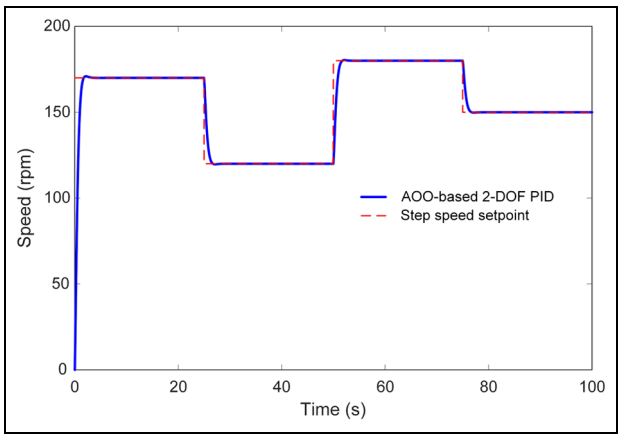



**Figure 8.** Time-domain analysis of the AOO-based 2-DOF PID controller under multiple step inputs.

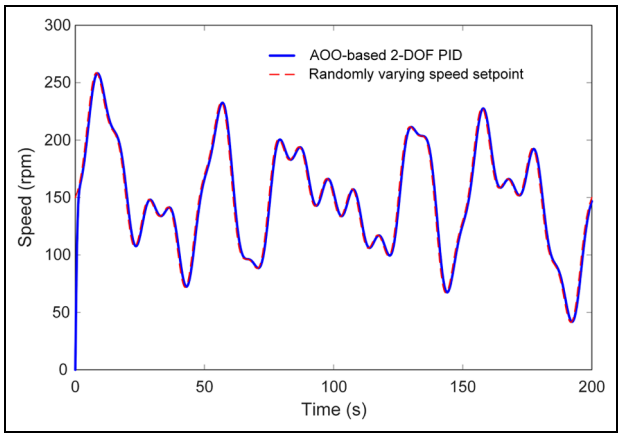



**Figure 9.** Time-domain analysis of the AOO-based 2-DOF PID controller under a randomly varying speed reference.

simulate the presence of sensor noise. The controller is anticipated to keep the speed tracking performance arbitrarily close to the ideal despite these disturbances.

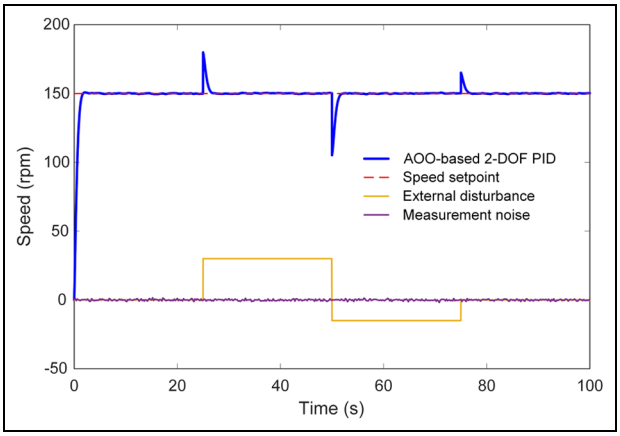



**Figure 10.** Time-domain analysis of the AOO-based 2-DOF PID controller in the presence of external disturbances and measurement noise.

The time-domain response results prove that the AOO-based 2-DOF PID controller can effectively eliminate the external disturbance inputs, while the output speed exhibits only small fluctuations. These transient dips and spikes, although visible, decay rapidly, and the system returns to the reference within a minimal recovery time. In addition, the effect of measurement noise is barely observable in the speed output, which suggests that the derivative filter structure in the 2-DOF PID design and the well-tuned control parameters play an important role in noise robustness. To sum up, these findings demonstrate that the proposed AOO-based 2-DOF PID can achieve good disturbance attenuation and noise robustness without deteriorating the steady-state performance and transient response. This highlights the usefulness of the proposed optimization framework for handling noise and uncertainty within the control loop, which are common challenges in practical motor drive applications.

## *Experimental results*

The feasibility and effectiveness of the proposed AOO-based 2-DOF PID control scheme in practice are verified by experiments on a laboratory-scale DC motor platform. The experimental setup is shown in Figure 11 and consists of a Pololu 37D×68L mm 12 V metal gearmotor with a 19:1 gear ratio controlled by an IBT-2 H-bridge motor driver. The unit is powered by a regulated DC power supply and connected to a host computer through Arduino-compatible microcontroller hardware.

Real-time signal generation and data acquisition, as well as controller deployment, are performed using MATLAB/Simulink and the Arduino Hardware Support Package. The proposed optimal control law is implemented through the Simulink environment and downloaded to an embedded controller, thus enabling intuitive computer-based implementation. For real-time implementation, the control algorithm runs with a fixed

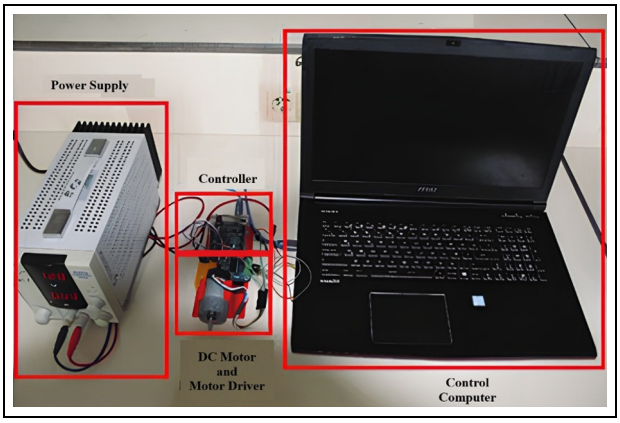



**Figure 11.** Experimental setup for real-time implementation of AOO-based 2-DOF PID controller.

sampling time via the Simulink–Arduino interface. Communication between the host and the embedded hardware occurs over a standard serial link, which introduces a small, constant delay that is negligible relative to the mechanical time constant of the DC motor. Because the AOO scheme is used only in the offline tuning step, the real-time control loop consists only of the 2-DOF PID computations, which guarantee reliable real-time execution with low computational burden. These features of the implementation clearly demonstrate the practical deployability of the proposed controller.

Figure 12 presents the real-time control model based on Simulink for the experimental test. The model combines the AOO-based 2-DOF PID controller with the identified DC motor model and the real motor hardware. The reference input is the same for the simulation model and the experimental loop for the purpose of comparison between the model outputs and real-time measurements. Two stages of processing are applied to the encoder feedback from the motor: count differentiation and low-pass filtering to acquire rotational speed, which is returned to the controller. The control command output from the experimental 2-DOF PID block is sent to the motor driver through the Arduino analog output interface, while a real-time pacer block is added to guarantee synchronous execution. This integrated design makes it possible to examine reference tracking performance, model–experiment agreement, and real-time control behavior in a uniform manner.

Figure 13 shows the time-domain speed responses of five different 2-DOF PID controllers to the reference signal. The experimental results show that the tracking performance and dynamic response of the AOO-based 2-DOF PID are superior. Although all controllers are successful in reaching the steady-state value, the AOO-based structure exhibits the shortest rise time and much lower overshoot among its counterparts. An expanded window from 2 to 3 s reveals that the AOO-based 2-DOF PID trajectory tracks the reference very closely without large oscillations. In comparison, other approaches have obvious oscillations or hysteresis in their transient performances. These results coincide with those from the simulations, demonstrating the potential to transfer AOO-based parameters directly from model-based tuning to real hardware implementation.

More results on the performance of the AOO-based 2-DOF PID are shown in Figure 14, where a complicated reference signal containing many step changes is used for the motor system. The experimental motor's response under the AOO-based 2-DOF PID is also compared with the model output obtained from simulation and the desired reference. The controller tracks $\omega c$ that varies at a high rate with a small steady-state error and recovers quickly from discontinuities. The close-up window also shows that the settling time is minimized together with overshoot suppression after an abrupt setpoint drop.

To sum up, the real-time experiments demonstrate that the proposed AOO-based 2-DOF PID controller

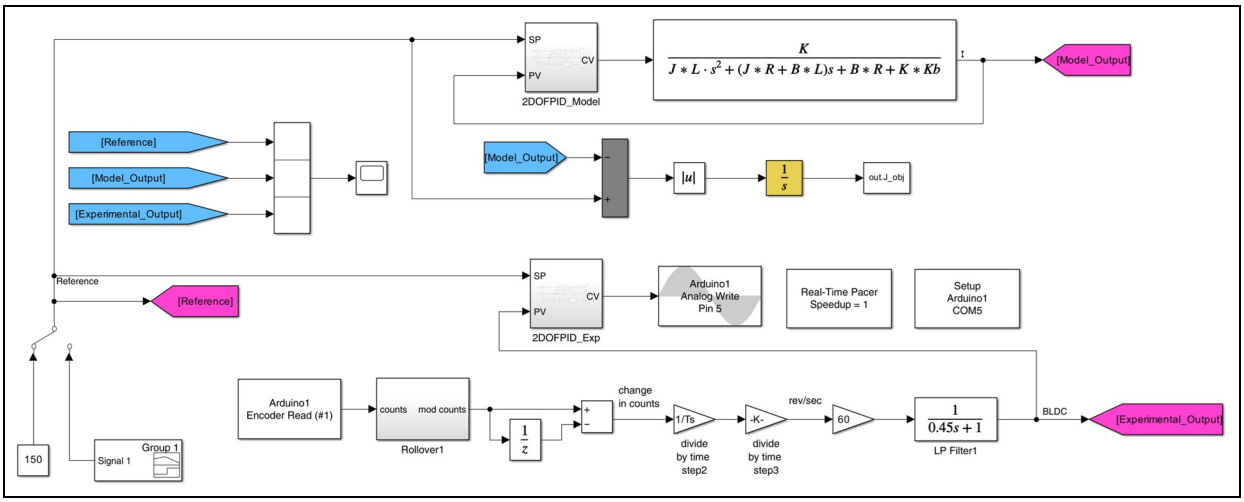



**Figure 12.** Developed Simulink Model.

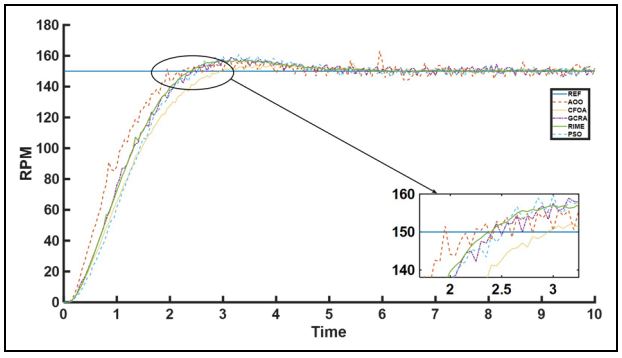



**Figure 13.** Comparative experimental time responses of 2-DOF PID controllers tuned by different optimization algorithms.

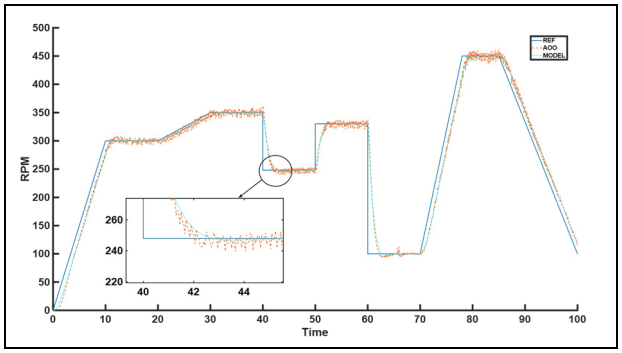



**Figure 14.** Experimental model tracking performance of AOO-based 2-DOF PID controller under complex reference profile.

can achieve superior performance in speed control under actual operating conditions. The transient performance is very good, and the system is robust to high-frequency variations and not sensitive to unmodeled dynamics or hardware implementation imperfections. These results confirm the practicality and usefulness of nature-inspired optimization methods with flexible PID-based structures for intelligent motor control.

Figure 14 shows how well the AOO-based 2-DOF PID controller can track a non-trivial, piecewise reference profile for a DC motor system in real time. The desired reference trajectory, experimental motor response, and identified model output are shown as blue solid, orange dotted, and green dashed lines, respectively. The response shows good tracking for both fast rise and fall transitions and steady state. The zoomed-in plot highlights the local tracking error at a sudden setpoint drop, illustrating that the controller is able to respond quickly and robustly to such abrupt changes without causing excessive overshoot or oscillation.

### *Discussion*

The conclusion of the investigation is that the AOO-based 2-DOF PID is a promising technique for high-performance DC motor speed control. AOO obtains better cost values more frequently than the other well-known metaheuristic algorithms, as illustrated by statistical metrics and boxplot distributions. This performance improvement is achieved due to the dynamic search behavior of AOO, which provides a good balance between exploration and exploitation, avoids premature convergence, and discovers globally optimal solutions for the controller parameters.

Regarding the speed of convergence, AOO rapidly converges to very low-cost values at the beginning of the searching process, indicating that it achieves better performance than the other methods in terms of both convergence stability and final objective value. Improved gain allocation and derivative filtering characteristics are achieved by the controller parameters tuned using AOO. The AOO-based 2-DOF PID affirms its feasibility for high-precision control applications by achieving the shortest rise time and settling time, minimal overshoot, and nearly zero steady-state error in the simulations. Also, the robustness of the proposed controller is proven through challenging reference tracking problems. When subjected to randomly changing reference speeds, the AOO-based 2-DOF PID is able to achieve accurate tracking of the reference signal with low tracking error and delay.

The simulation results are validated through an experimental testbed consisting of a physical DC motor system, where the real-time implementation of the AOO-based 2-DOF PID control attains the desired dynamic response. With the simulated and experimental outputs matching well with each other, the results fully support the practical implementation of the proposed method and confirm the proposed algorithm's generalization capability from system models to physical systems.

While the AOO algorithm has better control performance and convergence stability, it should be noted that there is a corresponding computational cost during the offline optimization process. Much like other nature-inspired population-based metaheuristic algorithms, AOO also requires multiple fitness evaluations over the iterations, increasing the total tuning time. This computational expense, however, is incurred only once during controller design, since AOO is not executed online. After optimization, only the time-invariant 2-DOF PID parameters are applied to the control loop, so there is almost no computational burden for online operation. Therefore, the achieved performance gains in tracking accuracy, robustness, and convergence reliability are worth the extra offline computational cost.

## Conclusions and perspectives for future research

In this paper, a new 2-DOF PID controller based on the AOO optimization algorithm is designed and tested for DC motor speed control. AOO, a nature-inspired

optimization algorithm based on the hygroscopic mechanism of ASL dispersal, is employed to find the optimal controller parameters that minimize a composite cost function including IAE and NPO. The results of extensive simulation and experimental tests validate that the AOO-based 2-DOF PID significantly outperforms other state-of-the-art metaheuristic algorithms such as CFOA, GCRA, RIME, and PSO in terms of a wide range of performance measures, including rise time, settling time, overshoot, steady-state error, convergence speed, and statistical consistency.

The controller achieves high accuracy in reference tracking tasks for both deterministic and stochastic input signals and shows strong robustness to external perturbations and measurement noise. In addition, the real-time experimental implementation of the control algorithm further strengthens the claim of its practicality and reliability beyond simulation constraints. These results demonstrate that the proposed method constitutes a promising approach for addressing modern control problems that require high accuracy and adaptability.

From this perspective, several opportunities for further research are clear. First, by formulating AOO within a multi-objective optimization framework, conflicting control objectives can be considered simultaneously. Second, real-time adaptive tuning algorithms may be developed based on AOO to update controller parameters online for systems with time-varying or unknown dynamics. Third, it is of interest to investigate the proposed approach in nonlinear, coupled, and/or MIMO systems, such as those in robotics, automotive, and renewable energy fields. Finally, comparative studies involving hybrid or ensemble metaheuristics could be conducted to reveal algorithmic synergistic effects that may further improve control performance in more complex operating environments.

Considering these findings, future research may explore the integration of offline optimization-based tuning with adaptive or hybrid parameter adjustment strategies. Recent studies have shown that combining nominal controller tuning with observer-assisted or disturbance-aware mechanisms can significantly enhance robustness in systems with strong nonlinearities and coupled dynamics.[34,35] In this context, extending the proposed AOO-based framework toward hybrid offline–online tuning architectures represents a promising direction for more complex and uncertain control applications.

## Acknowledgments

The authors would like to express their sincere gratitude to Lukas Prokop and Stanislav Misak for their exceptional supervision, project administration, and overall guidance throughout the course of this project. Their expertise and support were instrumental to its success.

## ORCID iDs

Davut Izci https://orcid.org/0000-0001-8359-0875
Ievgen Zaitsev https://orcid.org/0000-0003-3303-471X

## Ethics declaration

Not applicable.

## Consent to participate

Not applicable.

## Consent for publication

Not applicable.

## Author contributions

Gökhan Yüksek, Serdar Ekinci, Timur Lale: Conceptualization, Methodology, Software, Visualization, Investigation, Writing – Original draft preparation. Davut Izci, Rıdvan Fırat Çınar: Data curation, Validation, Supervision, Resources, Writing – Review & Editing. Mohit Bajaj, Vojtech Blazek, Ievgen Zaitsev: Project administration, Supervision, Resources, Writing – Review & Editing.

## Funding

The authors disclosed receipt of the following financial support for the research, authorship, and/or publication of this article: This research is funded by European Union under the REFRESH—Research Excellence For Region Sustainability and High-Tech Industries Project via the Operational Programme Just Transition under Grant CZ.10.03.01/00/22_003/0000048; in part by the National Centre for Energy II and ExPEDite Project a Research and Innovation Action to Support the Implementation of the Climate Neutral and Smart Cities Mission Project TN02000025; and in part by ExPEDite through European Union's Horizon Mission Programme under Grant 101139527.

## Declaration of conflicting interests

The authors declared no potential conflicts of interest with respect to the research, authorship, and/or publication of this article.

## Data availability statement

The datasets used and/or analyzed during the current study available from the corresponding author on reasonable request.*

## References

1. Jabari M, Ekinci S, Izci D, et al. Efficient DC motor speed control using a novel multi-stage FOPD(1 + PI) controller optimized by the Pelican optimization algorithm. *Sci Rep* 2024; 14: 22442.
2. Mohindru P. Review on PID, fuzzy and hybrid fuzzy PID controllers for controlling non-linear dynamic behaviour of chemical plants. *Artif Intell Rev* 2024; 57: 97.
3. Chen J. The application of PID control in DC motor control systems. *Appl Comput Eng* 2024; 81: 164–170.
4. Sharma M, Sharma S and Vajpai J. A novel approach to design and analyze fractional order PID controller for speed control of brushless DC motor. *Renew Energy Sustain Dev* 2024; 10: 279.

5. Fellag R and Belhocine M. Comparative analysis of PID, fuzzy PID, and ANFIS controllers for 2-DOF helicopter trajectory tracking: simulation and hardware implementation. *Arch Mech Eng* 2024; 71: 323–349. https://doi.org/10.24425/ame.2024.151331
6. Huba M, Bistak P, Vrancic D, et al. PID vs. model-based control for the double integrator plus dead-time model: noise attenuation and robustness aspects. *Mathematics* 2025; 13: 664.
7. Ekinci S, Izci D, Gider V, et al. Quadratic interpolation optimization-based 2DoF-PID controller design for highly nonlinear continuous stirred-tank heater process. *Sci Rep* 2025; 15: 16324.
8. Enad MH, Hassan RF, Khaleel Mahmoud AA, et al. Performance evaluation of a 2DOF_PID controller using metaheuristic optimization algorithms. *J Eur Syst Automat* 2024; 57: 709–715.
9. Olatunde AF, Dada AE and Mommoh JS. Advanced optimization of a two-degree-of-freedom PID controller for air pressure monitoring sensor using a multi-objective genetic algorithm. *Glob J Eng Technol Adv* 2025; 23: 045–076.
10. Desalegn B and Tamrat B. Overview of the PI (2DoF) algorithm in wind power system optimization and control. *Front Energy Res* 2024; 12: 1435455. https://doi.org/10.3389/fenrg.2024.1435455
11. Guras R, Strambersky R and Mahdal M. The PID and 2DOF control of the integral system - influence of the 2DOF parameters and practical implementation. *Meas Control* 2022; 55: 94–101.
12. Balaguer V, Gonzalez A, Garcia P, et al. Enhanced 2-DOF PID controller tuning based on an uncertainty and disturbance estimator with experimental validation. *IEEE Access* 2021; 9: 99092–99102.
13. Yüksek G. A novel delay-affected two degree of freedom PID controller using physics-inspired optimization for robust control applications. *Sci Rep* 2025; 16: 3453. https://doi.org/10.1038/s41598-025-33481-x
14. Shahi MNS, Orka NA and Ahmed A. 2DOF-PID-TD: a new hybrid control approach of load frequency control in an interconnected thermal-hydro power system. *Heliyon* 2024; 10: e36753.
15. Cevher B, Gümüş TE and Turan M. A single state sliding mode controller design using intelligent optimization algorithms for the chaotic WINDMI system. *Teh Vjesn* 2022; 29: 504–510.
16. Sharma A and Singh N. EV integrated two area power system for load frequency control by PSO Optimized 2DOF-PID controller under cyber attack. In: *2024 IEEE 4th International conference on sustainable energy and future electric transportation (SEFET)*, 2024, pp.1–6. IEEE.
17. Ch. Naga SK, Mohana D, Gangadhar Y, et al. Load frequency control of contemporary power system with honey badger algorithm tuned regulator. *i-manager's J Power Syst Eng* 2025; 12: 25.
18. Simhadri K, Mohanty B and Mohan Rao U. Optimized 2DOF PID for AGC of multi-area power system using Dragonfly algorithm. In: Malik H, Srivastava S, Sood Y, et al. (eds) *Applications of artificial intelligence techniques in engineering*. Springer, 2019, pp.11–22.
19. Ekinci S, Izci D and Hekimoğlu B. Optimal FOPID speed control of DC motor via opposition-based hybrid manta Ray foraging optimization and simulated annealing algorithm. *Arab J Sci Eng* 2021; 46: 1395–1409.
20. Kaveh M and Mesgari MS. Application of meta-heuristic algorithms for training neural networks and deep learning architectures: a comprehensive review. *Neural Process Lett* 2022; 55: 1–104.
21. Lale T, Yüksek G and Çınar RF. A novel hybrid metaheuristic for optimizing deep CNN hyperparameters to enhance heart disease prediction on a comprehensive merged dataset. *Cluster Comput* 2026; 29: 117.
22. Yüksek G. Optimized GDTP-XGBoost framework for wind power forecasting toward condition-based maintenance. *Eksploatacja i Niezawodnosc - Maint Reliab*. Epub ahead of print 21 November 2025. https://doi.org/10.17531/ein/214376
23. Halim AH, Ismail I and Das S. Performance assessment of the metaheuristic optimization algorithms: an exhaustive review. *Artif Intell Rev* 2021; 54: 2323–2409.
24. Yuksek G, Alkaya A and Mete AN. Implementation of linear active disturbance rejection control for a DC motor system. In: *2021 13th International conference on electrical and electronics engineering (ELECO)*, 2021, pp.119–123. IEEE.
25. Izci D, Ekinci S, Rizk-Allah RM, et al. Master–slave architecture enhanced and improved GBO tuned cascaded PI-PDN controller for speed regulation of DC motors. *Optim Control Appl Methods* 2025; 46: 2137–2152. https://doi.org/10.1002/oca.3313
26. Ekinci S, Izci D, Almomani MH, et al. Advanced control parameter optimization in DC motors and liquid level systems. *Sci Rep* 2025; 15: 1394.
27. Rojas JD, Arrieta O and Vilanova R. *Industrial PID controller tuning*. Springer International Publishing, 2021. https://doi.org/10.1007/978-3-030-72311-8
28. Izci D, Ekinci S and Hussien AG. An elite approach to re-design Aquila optimizer for efficient AFR system control. *PLoS One* 2023; 18: e0291788.
29. Jia H, Wen Q, Wang Y, et al. Catch fish optimization algorithm: a new human behavior algorithm for solving clustering problems. *Cluster Comput* 2024; 27: 13295–13332.
30. Agushaka JO, Ezugwu AE, Saha AK, et al. Greater cane rat algorithm (GCRA): a nature-inspired metaheuristic for optimization problems. *Heliyon* 2024; 10: e31629.
31. Su H, Zhao D, Heidari AA, et al. RIME: a physics-based optimization. *Neurocomputing* 2023; 532: 183–214.
32. Wang D, Tan D and Liu L. Particle swarm optimization algorithm: an overview. *Soft Comput* 2018; 22: 387–408.
33. Wang R-B, Hu R-B, Geng F-D, et al. The Animated Oat Optimization Algorithm: a nature-inspired metaheuristic for engineering optimization and a case study on Wireless Sensor Networks. *Knowl Based Syst* 2025; 318: 113589.
34. Zhong Y, Li D and Sun L. Multi-loop active disturbance rejection control for shell-and-tube heat exchanger: decoupled design and optimization. *Energy Convers Manag* 2025; 346: 120438.
35. Yuan S, Wang Z and Sun L. Modelica-based dynamic modeling and active disturbance rejection control for high-temperature PEMFC thermal management. *Appl Therm Eng* 2026; 283: 128852.